Supplementary information for

Elucidation of the high-voltage phase in the layered sodium ion battery cathode material P3-$Na_{0.5}Ni_{0.25}Mn_{0.75}O_2$

Jiatu Liu[1], Christophe Didier[2,3], Matthew Sale[1], Neeraj Sharma[4], Zaiping Guo[3], Vanessa E. Peterson[2,3], Chris D. Ling[1]

[1]School of Chemistry, The University of Sydney, Sydney, NSW 2006, Australia

[2]Australian Centre for Neutron Scattering, ANSTO, Sydney, NSW 2232, Australia

[3]Institute for Superconducting & Electronic Materials, University of Wollongong, Wollongong, NSW 2522, Australia

[4]School of Chemistry, UNSW Australia, Sydney, NSW 2052, Australia

1, Figures and tables

Table S 1. Rietveld-refinement results against XRPD data for the pristine P3-type $Na_{0.5}Ni_{0.25}Mn_{0.75}O_2$ powder synthesized at 650 °C corresponding to Figure 1(a) in the main article. The atomic displacement parameters (B_{iso}) for Mn and Ni were constrained to be the same. The Ni-Mn occupancies were fixed due to the very similar X-ray scattering factors of Mn and Ni.

Atoms in P3 phase	x/a	y/b	z/c	Fractional occupancy	B_{iso}
Na	0	0	0.1685(4)	0.259(3)	2.7(2)
O	0	0	0.6076(1)	1	0.23(5)
Mn	0	0	0	0.75	0.24(2)
Ni	0	0	0	0.25	0.24
Unit cell parameter	a/Å	c/Å	Weight ratio	Space group	R_B
P3 phase	2.8723(1)	16.896(1)	96.4(1)%	R-3m	2.38
NiO[1]	4.1681(4)		3.6(1)%	Fm-3m	2.24
R_p	5.18	R_{wp}	6.74	Gof	1.22
Stephen's Model on P3	ζ 0.56	S_{400} 34703	S_{202} 64	S_{004} 12501	S_{301} -2663

[1] Cairns, R W; Ott, E. X-Ray Studies of the System Nickel-Oxygen-Water. I. Nickelous Oxide and Hydroxide. Journal of the American Chemical Society, 1933, 55, 527-533

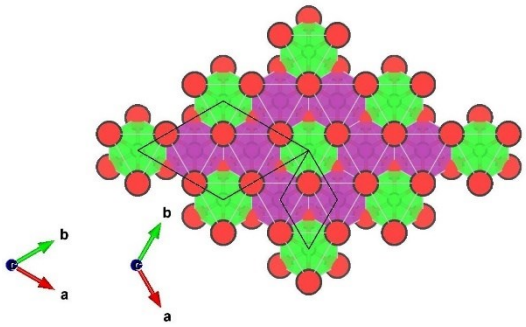

Figure S 1. The honeycomb layer ordering used in the stacking-fault model. Only one TMO_2 layer is shown. The Ni-rich site is green and the Mn-rich site is purple. Both the parent unit cell (*a=b≠c, α=β=90°, γ=120°*) and superstructure one-layer unit cell (*a'=b'=√3a≠c'=1/3c, α=β=90°, γ=60°*) are shown viewed along c axis. To fulfil the prismatic coordination environment for sodium ions between TMO_2 layers, the stacking vector can only be one of the following in the one-layer supercell basis:

(1/3, 0, 1), (-1/3, 1/3, 1), (0, -1/3, 1)

which leads to three types of layers with the same relative atomic configuration but different relative positions. The mutual transformation relationship of the three types of layers is summarized below:

To \ From	Type 1	Type 2	Type 3
Type 1	(1/3, 0, 1)	(0, -1/3, 1)	(-1/3, 1/3, 1)
Type 2	(-1/3, 1/3, 1)	(1/3, 0, 1)	(0, -1/3, 1)
Type 3	(0, -1/3, 1)	(-1/3, 1/3, 1)	(1/3, 0, 1)

The stacking faults models used sufficiently large number of layers of TMO_2 with the probability α(*i, j)* of finding type *j* layer next to type *i* layer as tabulated below:

To \ From	Type 1	Type 2	Type 3
Type 1	α11	α21	α31
Type 2	α12	α22	α32
Type 3	α13	α23	α33

In addition to the background, peak shape and crystallographic structure parameters, these stacking probabilities were refined in three different ways[2]:

Model 1, all probabilities equal to 1/3, α(*i, j*)=1/3. There is no extra refinable parameter.

Model 2, the probabilities of finding the same type at next layer are equivalent and the probabilities of finding different types at next layer are the same, α(*1, 1)* = α(*2, 2)* = α(*3, 3)* = *1 - 2*α(*i, j)* for *i≠j*. There is one extra refinable parameter.

Model 3, all probabilities are refinable.

---

[2] Liu, J., Yin, L., Wu, L., Bai, J., Bak, S.M., Yu, X., Zhu, Y., Yang, X.Q., and Khalifah, P.G. (2016). Quantification of Honeycomb Number-Type Stacking Faults: Application to Na3Ni2BiO6 Cathodes for Na-Ion Batteries. Inorg. Chem. 55, 8478–8492.

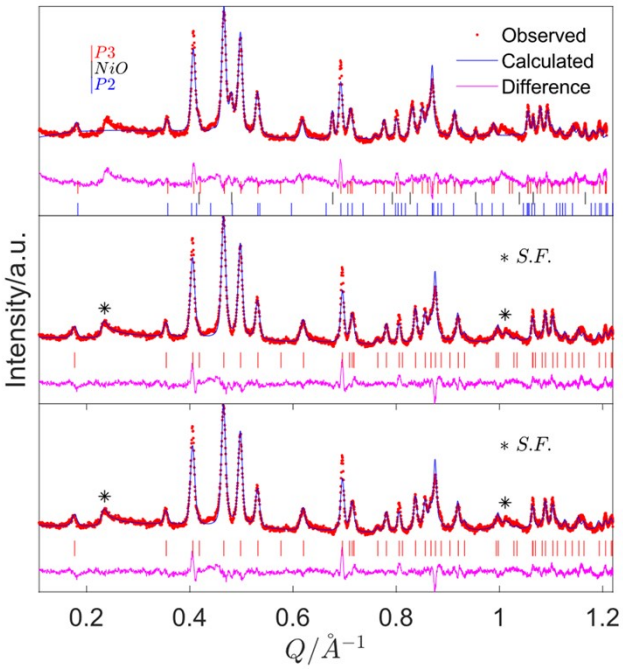

Figure S 2. NPD data and Rietveld-refined fits for P3-type $Na_{0.5}Ni_{0.25}Mn_{0.75}O_2$ synthesized at 650°C without and with stacking faults models using FullProf and FAULTS software respectively. From top to bottom: Rietveld refinement without stacking faults model; refinements using Model 1 with all stacking parameters equal to 1/3; and Model 2 with only one free stacking parameter.

Due to limitation of FAULTS software, the whole pattern was first refined without stacking faults using the FullProf software with three phases: P3, P2 and NiO. A small fraction of the P2 phase was tentatively added to the refinement model in the less-crystalline material for better FAULTS refinement. Peaks due to the minor NiO and P2 phases were manually subtracted from the original data before they were fed into FAULTS. The stacking-faults model satisfactorily addressed the most pronounced broadened peaks marked by asterisks (*). The overall goodness-of-fit was substantially improved by stacking-fault Model 3 as discussed in the main article. Refinements details are presented in the following tables.

Table S 2. NPD Rietveld refinement results of less-crystalline P3-type $Na_{0.5}Ni_{0.25}Mn_{0.75}O_2$ material without a stacking-fault model. The unit cell parameters of the P2 phase were kept the same as the P3 phase, i.e., $a_{P3} = a_{P2}$ and $c_{P3} = 3/2c_{P2}$, because the P2 phase reflections are broad and heavily overlapped with those of P3. Inclusion of the P2 phase in the refinement model accounts for the peak intensity at Q = 0.48 $Å^{-1}$. However, the P2 phase is not observed in XRD data in the main article and only serves to feed FAULTS with more pure data. B_{iso} for Mn and Ni were constrained to be the same, and the Na z position was set to 1/6 to avoid over-parameterization.

Atoms in P3 phase	x/a	y/b	z/c	Fractional occupancy	B_{iso}
Na	0	0	1/6	0.38(3)	6.9(4)
O	0	0	0.3913(2)	1	1.54(4)
Mn	0	0	0	0.78	2.5(2)
Ni	0	0	0	0.22(1)	2.5
Unit cell parameter	*a*/Å	*c*/Å	Weight ratio	Space group	R_B
P3 phase	2.8729(2)	16.9064(1)	88.3(2) %	R-3m	12.0
P2 phase[3]	-	-	8(1)%	P63/mmc	33.5
NiO	4.1597(3)		2.8(2)%	Fm-3m	10.6
R_p	4.8	R_{wp}	6.1	Gof	2.4
				χ^2	5.8

Table S 3. Comparison of different stacking-fault models. Ni/Mn mixing was set for the two Mn sites and one Ni sites in the honeycomb-ordered one-layer supercell. The refined compositions of the three models were all close to $Na_{0.6}Ni_{0.2}Mn_{0.8}O_2$, which differs slightly from our ICP results. The best goodness-of-fit obtained using Model 3 indicates that the stacking layer correlations extend further than next-nearest neighbors.

	Model 1	Model 2	Model 3
a/Å	4.9765(1)	4.9764(1)	4.9778(1)
c/Å	16.926(1)	16.926(1)	16.922(1)
Occ_Na	0.326(5)	0.329(5)	0.320(5)
B_{iso}_Na	5.6(2)	5.5(2)	6.7(2)
Occ_Ni_1	0.617(3)	0.620(3)	0.597(3)
Occ_Ni_2	0.030(2)	0.029(2)	0.006(2)
B_{iso}_TM	1.5(1)	1.5(1)	1.3(1)
z_O	0.0585(1)	0.0585(1)	0.0583(1)
B_{iso}_O	1.50(1)	1.50(2)	1.52(2)
$D_{Lorentzian}$	128(1)	129(1)	208(3)
α_{11} α_{12} α_{13}	1/3 1/3 1/3	0.46(2) 0.27 0.27	0.3(2) 0.3(2) 0.4(3)
α_{21} α_{22} α_{23}	1/3 1/3 1/3	0.27 0.46 0.27	0.4(3) 0.2(2) 0.6(2)
α_{31} α_{32} α_{33}	1/3 1/3 1/3	0.27 0.27 0.46	0.3(1) 0.3(1) 0(1)
R_p	4.23	4.23	4.04
χ^2	4.40	4.40	3.74

[3] Yabuuchi, N.; Kajiyama, M.; Iwatate, J.; Nishikawa, H.; Hitomi, S.; Okuyama, R.; Usui, R.; Yamada, Y.; Komaba, S. P2-Type Nax [Fe1/2 Mn1/2[O2 Made from Earth-Abundant Elements for Rechargeable Na Batteries. *Nat. Mater.* **2012**, *11*, 512–517.

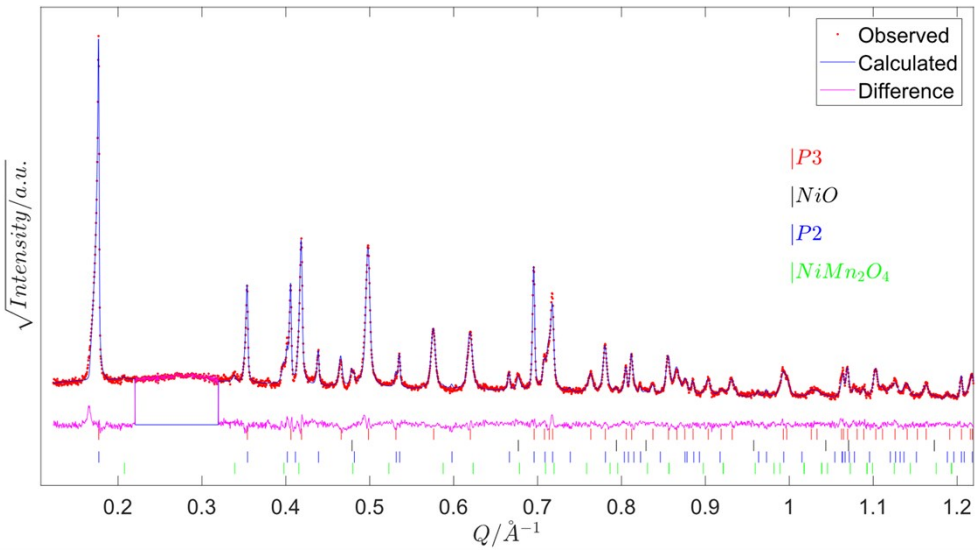

Figure S 3. Lab XRPD pattern and Rietveld refinement of the highly crystalline P3-type $Na_{0.5}Ni_{0.25}Mn_{0.75}O_2$ powder synthesized at 800 °C with P2-type, NiO, and $NiMn_2O_4$ impurities. The latter two are electrochemically inactive. The small hump around 0.3 $Å^{-1}$ due to the glass capillary was excluded from the refinement.

Table S 4. Rietveld-refinement results against XRPD data for the highly crystalline P3-type $Na_{0.5}Ni_{0.25}Mn_{0.75}O_2$ powder synthesized at 800 °C. B_{iso} for Mn and Ni were constrained to be the same.

Atoms in P3 phase	x/a	y/b	z/c	Fractional occupancy	B_{iso}
Na	0	0	0.1684(5)	0.21(4)	1.4(2)
O	0	0	0.6062(2)	1	0.1(6)
Mn	0	0	0	0.75	0.07(2)
Ni	0	0	0	0.25	0.07
Unit cell parameter	*a*/Å	*c*/Å	Weight ratio	Space group	R_B
P3 phase	2.8741(1)	16.943(1)	84.8(2) %	R-3m	2.42
P2 phase	2.8744(2)	11.285(1)	11.7%	P63/mmc	3.29
NiO	4.178(1)		0.7%	Fm-3m	1.50
$NiMn_2O_4$[4]	8.338(2)		2.8%	Fd-3m	4.00
R_p	7.04	R_{wp}	9.50	Gof	1.27
Stephen's Model on P3	Z 0.48	S_{400} 4422	S_{202} 9	S_{004} 7688	S_{301} -2237

[4] Meenakshisundaram, A.; Srinivasan, V.; Gunasekaran, N. Distribution of metal ions in transition metal manganites A Mn2 O4 A= Co, Ni, Cu, or Zn. Physica Status Solidi, Sectio A: Applied Research, 1982, 69, 15-19

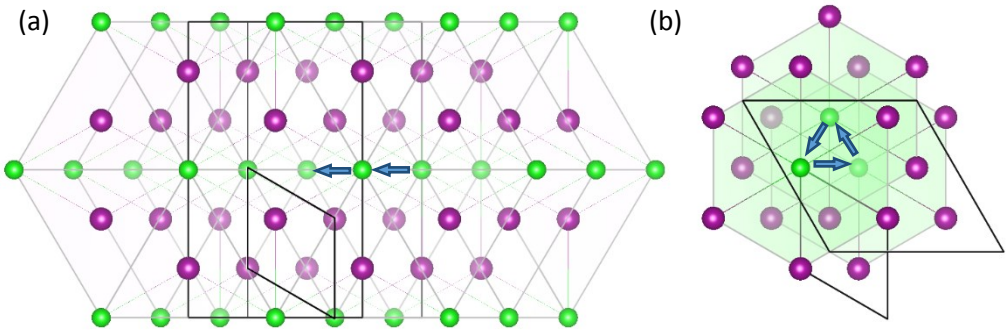

Figure S 4. The most best "small box" models we employed to address the "stacking faults" peaks and their relationship with parent P3 type structure in space group R-3m. Only nickel (green) and manganese (purple) ions are shown to emphasize the honeycomb ordering. (a) Monoclinic model in space group C2/m where the stacking vector is always one of the three aforementioned stacking vectors. (b) Trigonal model in space group $P3_112$ where the stacking vector moves among the three aforementioned stacking vectors. The crystallographic parameters are kept the same with the parent structure in the following affine transformation:

P3 (a b c P_0) →Monoclinic model (a_1 b_1 c_1 Q_1):

$$\begin{pmatrix} a_1 \\ b_1 \\ c_1 \\ Q_1 \end{pmatrix} = \begin{pmatrix} 2 & 1 & 0 & 0 \\ 0 & 3 & 0 & 0 \\ -2/3 & -1/3 & 1/3 & 0 \\ 0 & -1/2 & 0 & 1 \end{pmatrix} \begin{pmatrix} a \\ b \\ c \\ P_0 \end{pmatrix}$$

P3 (a b c P_0) →Trigonal model (a_2 b_2 c_2 Q_2):

$$\begin{pmatrix} a_2 \\ b_2 \\ c_2 \\ Q_2 \end{pmatrix} = \begin{pmatrix} 2 & 1 & 0 & 0 \\ -1 & 1 & 0 & 0 \\ 0 & 0 & 1 & 0 \\ 1/3 & 1/3 & 0 & 1 \end{pmatrix} \begin{pmatrix} a \\ b \\ c \\ P_0 \end{pmatrix}$$

where P_0 is the origin of R-3m structure, Q_1 that of C2/m structure and Q_2 that of P3 12 structure. Only the scale factor and one Lorentzian peak shape parameter are refined for both "small box" phases.

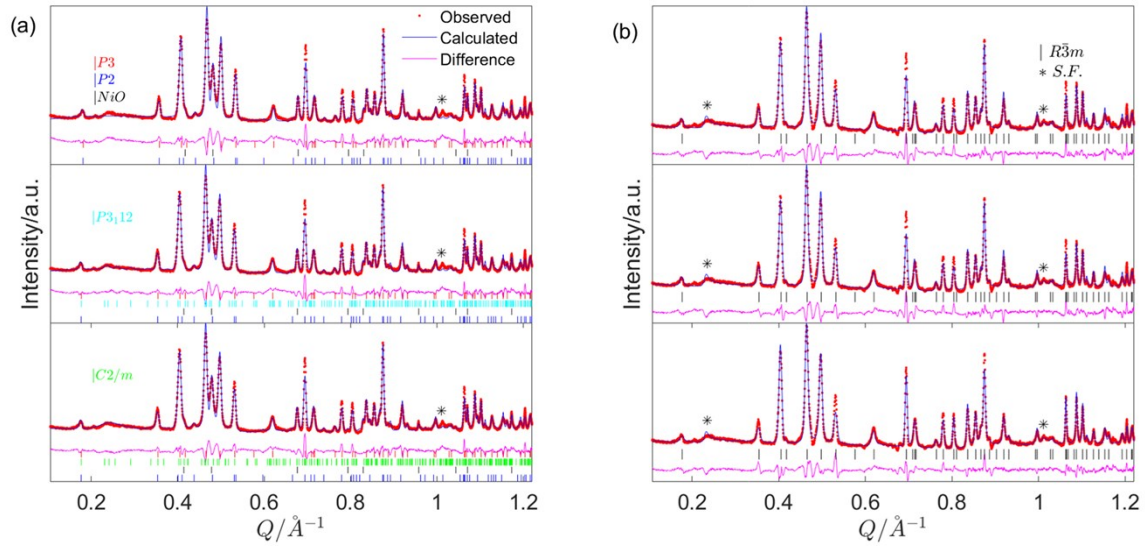

Figure S 5. Different refinement models we used to fit the NPD data of the highly crystalline P3-type $Na_{0.5}Ni_{0.25}Mn_{0.75}O_2$ sample synthesized at 800°C. (a) Rietveld refinements from top to bottom: without any stacking model or aforementioned "small box" phase; using a trigonal "small box" phase; and using a monoclinic "small box" phase. Both $P3_112$ and C2/m seem to address the first broadened extra peak around 0.23 $Å^{-1}$ satisfactorily, but not the second broadened extra peak around 1.01 $Å^{-1}$ marked by an asterisk (*), which implies that high temperature induces the development of small domains of ordered phases scattered in the parent matrix. (b) Results of refinements from top to bottom: using stacking Model 1 with all stacking parameters equals to 1/3; using Model 2 with only one free stacking parameter; and using Model 3 with all free stacking parameters. Contrary to the results in (a), all three stacking-fault models address the second but not the first broadened extra peak (marked *) satisfactorily. The best solution might lie somewhere between the "small box" model and the stacking fault-model, the development and details of which is beyond the scope of this research.

Table S 5. NPD Rietveld refinement results of the highly crystalline P3-type $Na_{0.5}Ni_{0.25}Mn_{0.75}O_2$ sample without a stacking-fault model. The B_{iso} parameters of Mn and Ni are constrained to be the same. The Na z position is set to 1/6 due to the strong correlation with its occupancy.

Atoms in P3 phase	x/a	y/b	z/c	Fractional occupancy	B_{iso}
Na	0	0	1/6	0.360(4)	5.2(3)
O	0	0	0.3923(2)	1	1.22(3)
Mn	0	0	0	0.795	1.3(1)
Ni	0	0	0	0.205(1)	1.3
Unit cell parameter	*a*/Å	*c*/Å	Weight ratio	Space group	R_B
P3 phase	2.8773(1)	16.9057(7)	79(1) %	R-3m	9.2
P2 phase	2.8796(2)	11.290(1)	17.6(7)%	P63/mmc	17.5
NiO	4.1765(2)		3.3(1)%	Fm-3m	16.3
R_p	6.0	R_{wp}	7.7	Gof	4.2
				χ^2	17.4

Table S 6. Comparison of R_p and χ^2 among refinements using different models for the highly crystalline P3-type $Na_{0.5}Ni_{0.25}Mn_{0.75}O_2$ sample synthesized at 800°C.

	Rietveld refinement	"small box" model		Stacking faults model		
		$P3_112$	C2/m	Model 1	Model 2	Model 3
R_p	6.0	5.7	5.4	5.6	5.6	4.6
χ^2	17.4	16.1	14.4	13.3	13.4	9.3

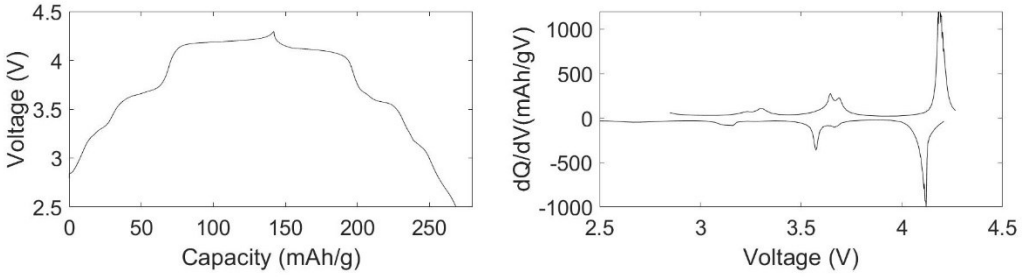

Figure S 6. The first cycle charging/discharging curve and corresponding dQ/dV curve of coin cell made up of highly crystalline P3-type $Na_{0.5}Ni_{0.25}Mn_{0.75}O_2$ sample synthesized at 800°C. Three pairs of redox peaks similar to those of P3-type $Na_{0.5}Ni_{0.25}Mn_{0.75}O_2$ sample synthesized at 650°C are well resolved.

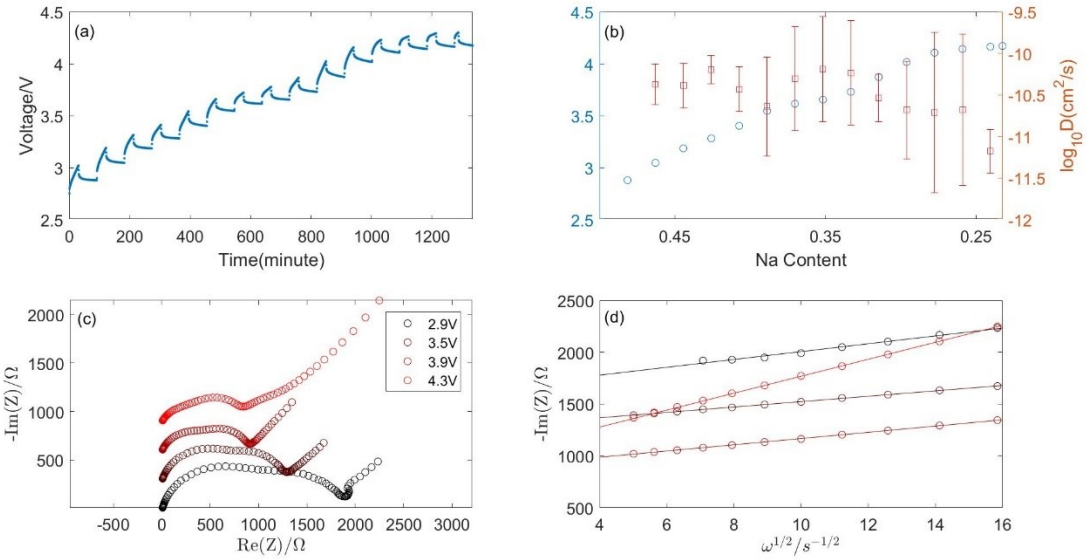

Figure S 7. (a) The GITT curve of the charging process of P3-type $Na_{0.5}Ni_{0.25}Mn_{0.75}O_2$ sample synthesized at 650°C after 20 cycles at 10 mAh/g and (b) calculated diffusion coefficients at each titration steps. (c) The EIS data at different state of charge for the same material after 20 cycles and (d) linear fit of the low frequency data points, from which the diffusion coefficients are calculated to be $10^{-13.8}$, $10^{-13.1}$, $10^{-13.1}$, $10^{-13.9}$ cm^2/s for 2.9, 3.5, 3.9, 4.3 V. One conspicuous difference between the EIS data of the fresh sample and that of the cycled sample is that the one semicircle of the fresh sample developed into at least two semicircles of the cycled sample in the high-medium frequency region, compared with Figure 2 in the main text. This indicates the formation of at least one extra interface that is rate-limiting. Of note is the absolute value of the impedance is not comparable between different coin cells.

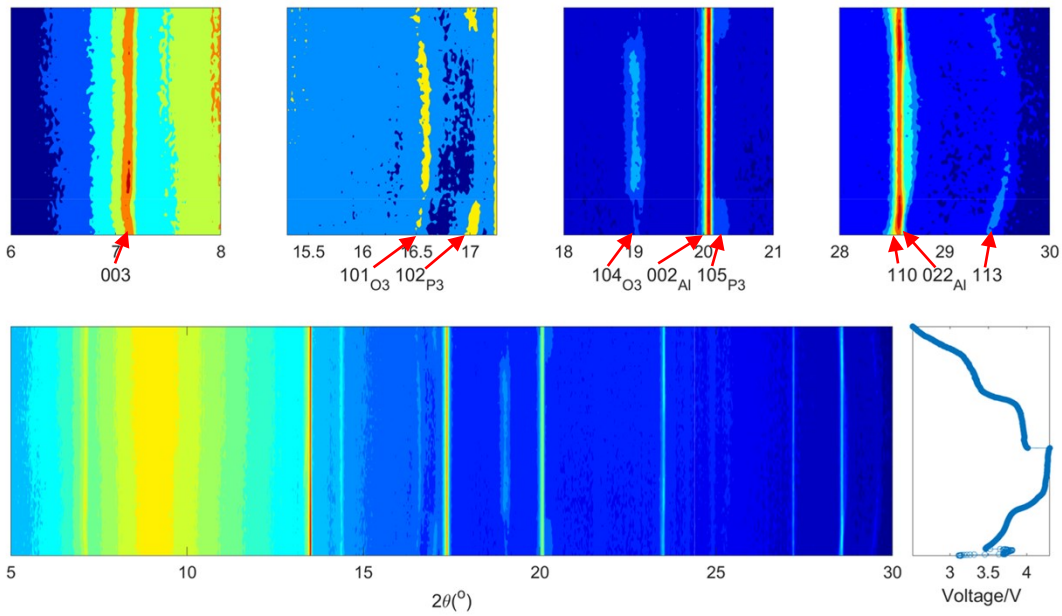

Figure S 8. *In situ* PXRD (Mo Kα, λ = 0.71073 Å) data of the coin cell made from the highly crystalline P3-type $Na_{0.5}Ni_{0.25}Mn_{0.75}O_2$ sample synthesized at 800°C charged at 10 mA/g in 4.3-2.5 V. The area of observation is covered and sealed by Kapton film. Only the P3→O3 transition is observed, probably due to the lack of sufficient mechanical compression in the area of observation.

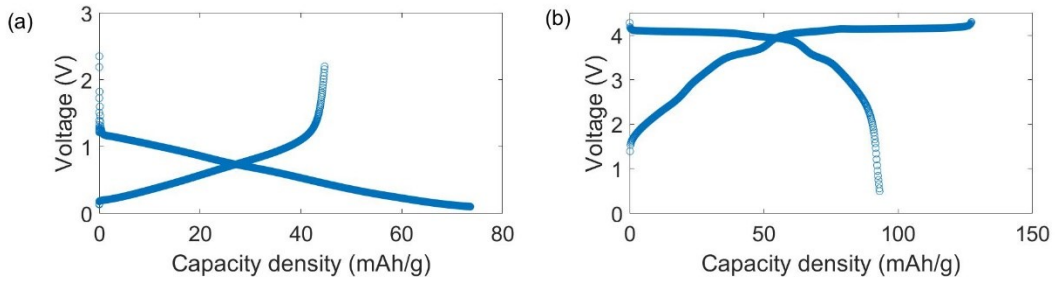

Figure S 9. First cycle of hard carbon electrode vs. sodium pellets at 10 mA/g (a) and first cycle of $Na_{0.5}Ni_{0.25}Mn_{0.75}O_2$-hard carbon coin cell at 10 mA/g with respect to the positive electrode (b).

Table S 7. Rietveld-refinement results against the initial *in situ* NPD pattern (a) in Figure 3 of the main article. B_{iso} parameter were all fixed to 1.0 and the z position and of fractional occupancy Na was fixed to avoid over-parameterization. Only the unit cell parameters and weight fractions were refined for the P2 phase and aluminium.

Atoms in P3 phase	x/a	y/b	z/c	Occupancy	B_{iso}
Na	0	0	1/6	0.25	1.0
O	0	0	0.6063(5)	1	1.0
Mn	0	0	0	0.75	1.0
Ni	0	0	0	0.25	1.0
Unit cell parameter	a/Å	c/Å	Weight ratio	Space group	R_B
P3 phase	2.8724(3)	16.918(4)	73%	R-3m	0.12
Aluminium	4.050(1)		13%	Fm-3m	0.16
P2 phase	2.878(2)	11.43(1)	14%	P63/mmc	0.18
R_p	0.31	R_{wp}	0.39	χ^2	1.0

Table S 8. Refinement result against the *in situ* NPD pattern (b) in Figure 3 of the main article. Only the unit cell parameters and weight fractions were refined for the P3 phase. All parameters for P2 and aluminium were fixed.

Atoms in O3 phase	x/a	y/b	z/c	Fractional occupancy	B_{iso}
Na	0	0	1/6	0.15	1.0
O	1/3	2/3	0.3935(4)	1	1.0
Mn	0	0	0	0.75	1.0
Ni	0	0	0	0.25	1.0
Unit cell parameter	a/Å	c/Å	Weight ratio	Space group	R_B
O3 phase	2.8555(3)	16.958(3)	54%	R-3m	0.08
P3 phase	2.872(3)	16.34(4)	19%	R-3m	0.11
R_p	0.31	R_{wp}	0.41	χ^2	1.1

Table S 9. Refinement result against the *in situ* NPD pattern (c) in Figure 3 of the main article. Only the unit cell parameters and weight fractions were refined for the P3 and O3 phases. The persistent presence of a P3 phase indicates that some amount of it is inactive, possibly due to the pouch cell assembly.

Atoms in O3s phase	x/a	y/b	z/c	Fractional occupancy	B_{iso}
O	1/3	2/3	0.4000(4)	1	1.0
Mn	0	0	0	0.75	1.0
Ni	0	0	0	0.25	1.0
Unit cell parameter	a/Å	c/Å	Weight ratio	Space group	R_B
O3s phase	2.8543(4)	13.272(4)	41%	R-3m	0.05
P3 phase	2.863(2)	17.17(2)	20%	R-3m	0.10
O3 phase	2.848(1)	16.59(3)	7%	R-3m	0.10
Rp	0.28	Rwp	0.34	χ2	1.0

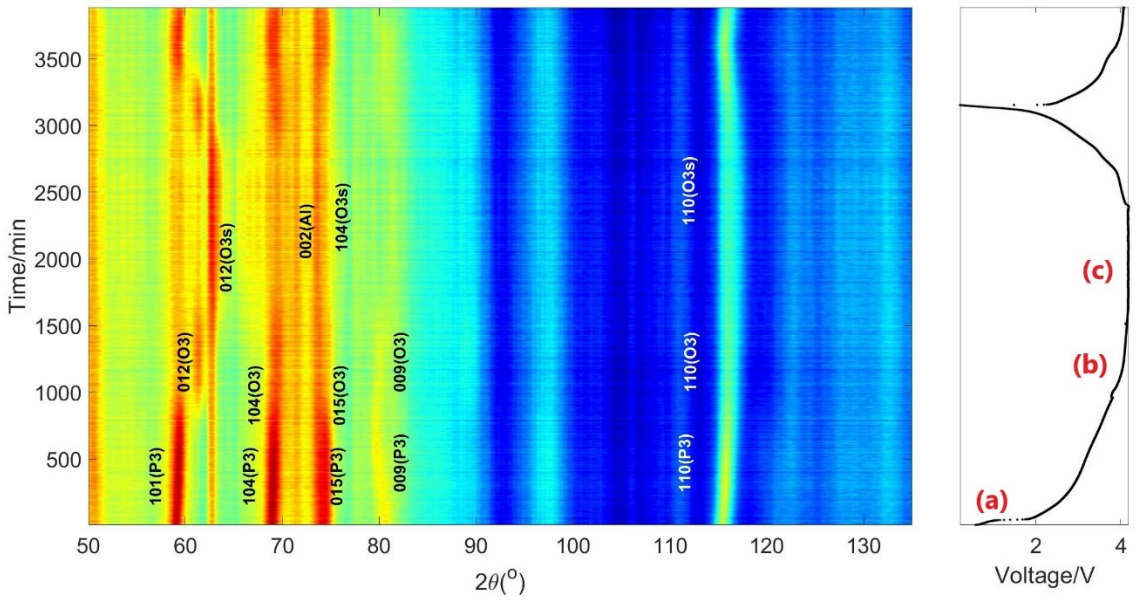

Figure S 10. *In situ* NPD contour plot of the P3-type $Na_{0.5}Ni_{0.25}Mn_{0.75}O_2$-hard carbon pouch cell cycled at 10 mA/g between open circuit voltage and 4.16 V. This pouch never reached 4.3 V, probably due to moisture penetration. Nevertheless, the two-phase transformations from P3 to O3 to O3s are observed. Intensity is highest in red and lowest in blue.

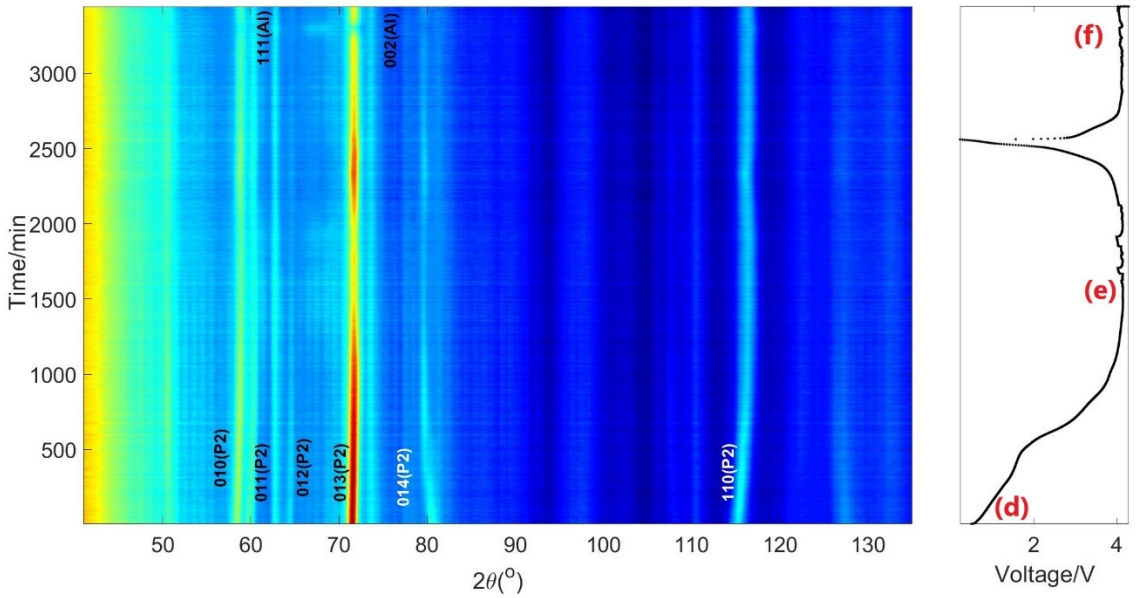

Figure S 11. *In situ* NPD contour plot of P2-type $Na_{0.5}Ni_{0.25}Mn_{0.75}O_2$-hard carbon pouch cell cycled at 10 mA/g between open circuit voltage and 4.1 V. This pouch never reached 4.3 V, again probably due to moisture infiltration into the pouch. The cycling curve shows typical staggered behavior above 4 V indicating the presence of water or water-assisted decomposition. Nevertheless, the intensity changes of the 013 reflection of P2-type is observed in the high-voltage region. Intensity is highest in red and lowest in blue.

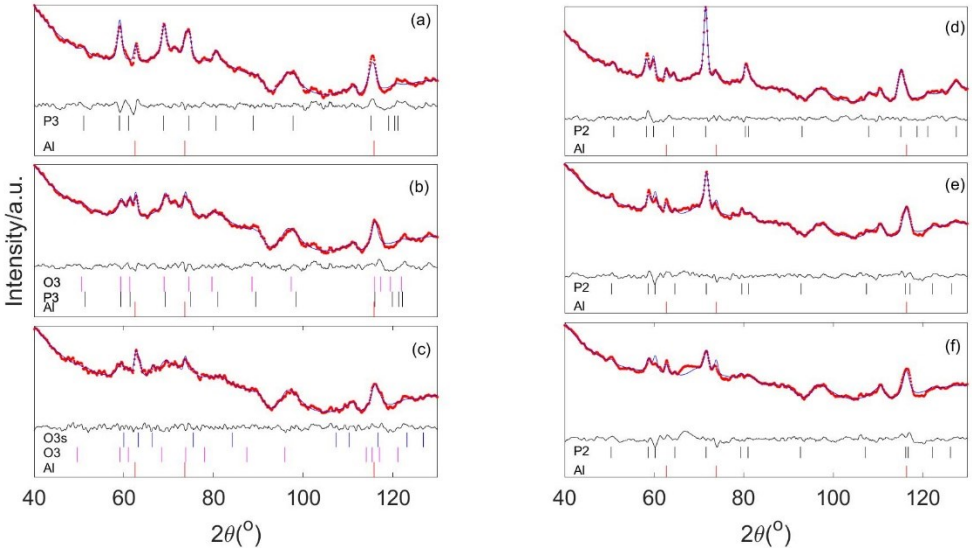

Figure S 12. Rietveld refinement results for NPD data denoted in Figure S 10 and Figure S 11, i.e. the beginning (a), mid-stage (b) and final stage (c) of the charging process for the pouch cell made up of the P3-type $Na_{0.5}Ni_{0.25}Mn_{0.75}O_2$ sample synthesized at 650°C, and the beginning (d), the final stage in the first cycle (e) and in the second cycle (f) for the pouch cell made up of the P2-type $Na_{0.5}Ni_{0.25}Mn_{0.75}O_2$ sample synthesized at 900°C. Of note is that the second cycle (f) seems to reach a higher state of charge than the first cycle (e), as manifested in the sharper decrease of 013 reflection around 71° and emergence of a hump just before 013 reflection. Nevertheless both pouch cells were compromised by moisture infiltration. The quality of both data is inferior than that of the highly crystalline P3-type $Na_{0.5}Ni_{0.25}Mn_{0.75}O_2$ sample synthesized at 800°C. Red: observed. Blue: Rietveld fitted. Black: mismatch between the observed data and the fitted.

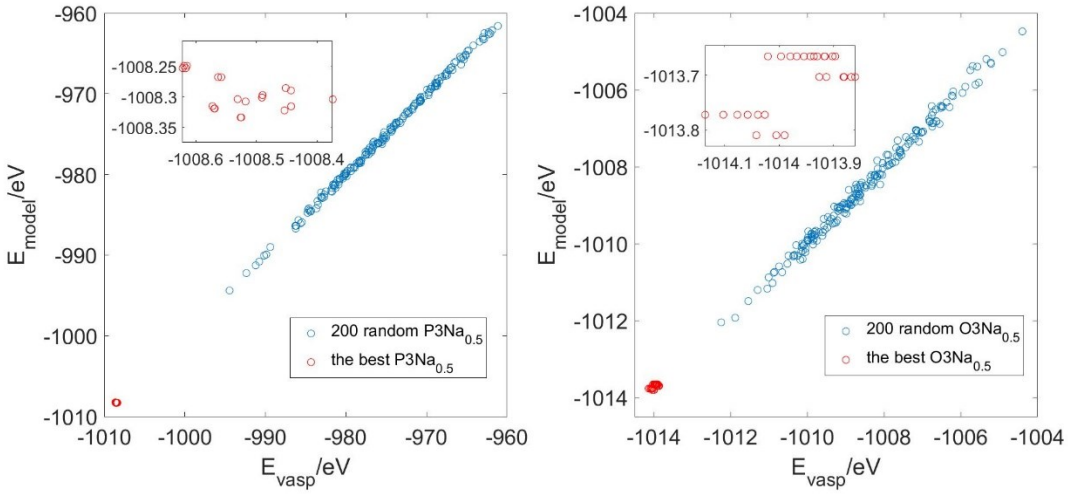

Figure S 13. Modelled vs. calculated energies (prior to relaxation) of random vs. the best sodium configurations of P3-type and O3-type $Na_{0.5}Ni_{0.25}Mn_{0.75}O_2$, as predicted by a linear model,

$$E = X \cdot \beta + \varepsilon.$$

For P-type structures, $X_P = (1,x_1,x_2,\ldots,x_8)$. (x_1,x_2,x_3,x_4) are the numbers of the 1st-nearest to the 4th-nearest in-plane Na-Na interactions. (x_5,x_6,x_7,x_8) are the numbers of the 1st-nearest to the 4th-nearest interlayer Na-Ni interactions. For O-type structures, $X_O = (1,x_1,x_2,x_3)$. (x_1) is the number of the 1st-nearest in-plane Na-Na interaction. (x_2,x_3) are the numbers of the 1st-nearest to the 2nd-nearest interlayer Na-Ni interactions. Including more items (x) does not improve the model significantly. The coefficient values for P3-type models are β_P = (-1005.9940, 3.7006, 0.4809, 0.2665, -0.3771, -0.2461, -0.1271, -0.1322) and for O3 type models are β_O = (-1010.6492, 0.4673, -0.2148, -0.1613). The error of the energy σ_E determined from statistical fitting is propagated as: $\sigma_E^2 = \sum_{i,j}\left(\frac{\partial f}{\partial \beta_i}\right)\left(\frac{\partial f}{\partial \beta_j}\right)\sigma_{ij}$. The variance-covariance of β is σ_{ij}. The error predicted for one sigma is less than 0.15 eV for P type and 0.05 eV for O type structures *per* 48 formula units. The actual difference between energies calculated without relaxation and predicted are 0.2 eV for P-type and 0.18 eV for O-type structures per 48 formula units as shown in the inset-plots. However, the energy predicted by the linear model is adequate because the smallest energy difference given by Figure 6 in the main article is 0.01 eV *per* formula unit, which is larger than the error associated with the linear model.

P3Na1/2

1 F= -.10139901E+04 E0= -.10139900E+04 d E =-.215310E-03 mag= 132.0000
1 F= -.10140418E+04 E0= -.10140418E+04 d E =-.411657E-04 mag= 131.9999
1 F= -.10140052E+04 E0= -.10140050E+04 d E =-.316647E-03 mag= 132.0001
1 F= -.10140262E+04 E0= -.10140261E+04 d E =-.105549E-03 mag= 131.9999
1 F= -.10140579E+04 E0= -.10140578E+04 d E =-.152211E-03 mag= 132.0000
1 F= -.10140391E+04 E0= -.10140389E+04 d E =-.393289E-03 mag= 132.0003
1 F= -.10140767E+04 E0= -.10140766E+04 d E =-.237269E-03 mag= 131.9989
1 F= -.10141359E+04 E0= -.10141357E+04 d E =-.294103E-03 mag= 132.0002
1 F= -.10141026E+04 E0= -.10141024E+04 d E =-.468245E-03 mag= 132.0000
1 F= -.10138604E+04 E0= -.10138603E+04 d E =-.268880E-03 mag= 132.0001
1 F= -.10139133E+04 E0= -.10139133E+04 d E =-.695043E-04 mag= 132.0001
1 F= -.10138675E+04 E0= -.10138673E+04 d E =-.264493E-03 mag= 132.0000
1 F= -.10138969E+04 E0= -.10138969E+04 d E =-.837589E-04 mag= 132.0000
1 F= -.10139301E+04 E0= -.10139301E+04 d E =-.863404E-04 mag= 132.0000
1 F= -.10139020E+04 E0= -.10139018E+04 d E =-.341621E-03 mag= 132.0001
1 F= -.10139363E+04 E0= -.10139356E+04 d E =-.140116E-02 mag= 132.0000
1 F= -.10139966E+04 E0= -.10139962E+04 d E =-.793693E-03 mag= 132.0000
1 F= -.10139543E+04 E0= -.10139534E+04 d E =-.170713E-02 mag= 132.0000
1 F= -.10138807E+04 E0= -.10138805E+04 d E =-.458862E-03 mag= 132.0001
1 F= -.10139262E+04 E0= -.10139262E+04 d E =-.122674E-03 mag= 132.0000
1 F= -.10138817E+04 E0= -.10138815E+04 d E =-.409755E-03 mag= 131.9991
1 F= -.10139168E+04 E0= -.10139167E+04 d E =-.328869E-03 mag= 132.0002
1 F= -.10139426E+04 E0= -.10139425E+04 d E =-.203611E-03 mag= 132.0000
1 F= -.10139161E+04 E0= -.10139158E+04 d E =-.581407E-03 mag= 131.9999
1 F= -.10139676E+04 E0= -.10139673E+04 d E =-.475693E-03 mag= 132.0000
1 F= -.10140207E+04 E0= -.10140204E+04 d E =-.486255E-03 mag= 132.0000
1 F= -.10139796E+04 E0= -.10139794E+04 d E =-.516477E-03 mag= 132.0000

O3Na1/2

1 F= -.10085256E+04 E0= -.10085251E+04 d E =-.931381E-03 mag= 131.9999
1 F= -.10085693E+04 E0= -.10085687E+04 d E =-.110664E-02 mag= 132.0000
1 F= -.10085731E+04 E0= -.10085725E+04 d E =-.114438E-02 mag= 131.9999
1 F= -.10084429E+04 E0= -.10084427E+04 d E =-.409533E-03 mag= 132.0001
1 F= -.10084912E+04 E0= -.10084909E+04 d E =-.606977E-03 mag= 131.9999
1 F= -.10084906E+04 E0= -.10084901E+04 d E =-.891918E-03 mag= 131.9999
1 F= -.10085583E+04 E0= -.10085579E+04 d E =-.779616E-03 mag= 131.9999
1 F= -.10086168E+04 E0= -.10086164E+04 d E =-.807193E-03 mag= 131.9998
1 F= -.10086161E+04 E0= -.10086144E+04 d E =-.328075E-02 mag= 132.0009
1 F= -.10085264E+04 E0= -.10085259E+04 d E =-.974805E-03 mag= 131.9999
1 F= -.10085700E+04 E0= -.10085695E+04 d E =-.101118E-02 mag= 131.9999
1 F= -.10085733E+04 E0= -.10085726E+04 d E =-.121692E-02 mag= 131.9999
1 F= -.10084432E+04 E0= -.10084430E+04 d E =-.462095E-03 mag= 132.0002
1 F= -.10084913E+04 E0= -.10084911E+04 d E =-.526536E-03 mag= 131.9999
1 F= -.10084903E+04 E0= -.10084898E+04 d E =-.944142E-03 mag= 131.9999
1 F= -.10085636E+04 E0= -.10085632E+04 d E =-.858161E-03 mag= 131.9997
1 F= -.10086219E+04 E0= -.10086215E+04 d E =-.776825E-03 mag= 131.9998
1 F= -.10086207E+04 E0= -.10086192E+04 d E =-.317019E-02 mag= 132.0002
1 F= -.10084564E+04 E0= -.10084538E+04 d E =-.520970E-02 mag= 131.9998
1 F= -.10085196E+04 E0= -.10085179E+04 d E =-.335729E-02 mag= 131.9999
1 F= -.10085315E+04 E0= -.10085310E+04 d E =-.963174E-03 mag= 131.9999
1 F= -.10083762E+04 E0= -.10083742E+04 d E =-.396914E-02 mag= 132.0001
1 F= -.10084443E+04 E0= -.10084431E+04 d E =-.237014E-02 mag= 131.9999
1 F= -.10084521E+04 E0= -.10084518E+04 d E =-.582400E-03 mag= 132.0004
1 F= -.10084763E+04 E0= -.10084727E+04 d E =-.718011E-02 mag= 131.9999
1 F= -.10085538E+04 E0= -.10085513E+04 d E =-.508566E-02 mag= 131.9999
1 F= -.10085609E+04 E0= -.10085591E+04 d E =-.359173E-02 mag= 131.9999

Box S 1. Calculated energies and total magnetic moment of the best Na configurations in P3-type and O3-type $Na_{0.5}Ni_{0.25}Mn_{0.75}O_2$ (4x4x1 supercell, 48 formula) corresponding to those in Figure S 13. The total magnetic moment of each structure keeps at 2x12(Ni)+3x36(Mn)=132 (corresponding to ferromagnetic), irrelevant to the sodium configuration and P3/O3 type. The total magnetic moments of the final P-O series structures are 132, 129, 126, 123, 120, 117, 108 for 48 formula P3Na1/2, P3Na7/16, P3Na3/8, O3Na5/16, O3Na1/4, O3Na3/16, O3Na0, which reflects the fractional desodiation process with the number of unpaired electrons reduced. All structures are stable in ferromagnetic state.

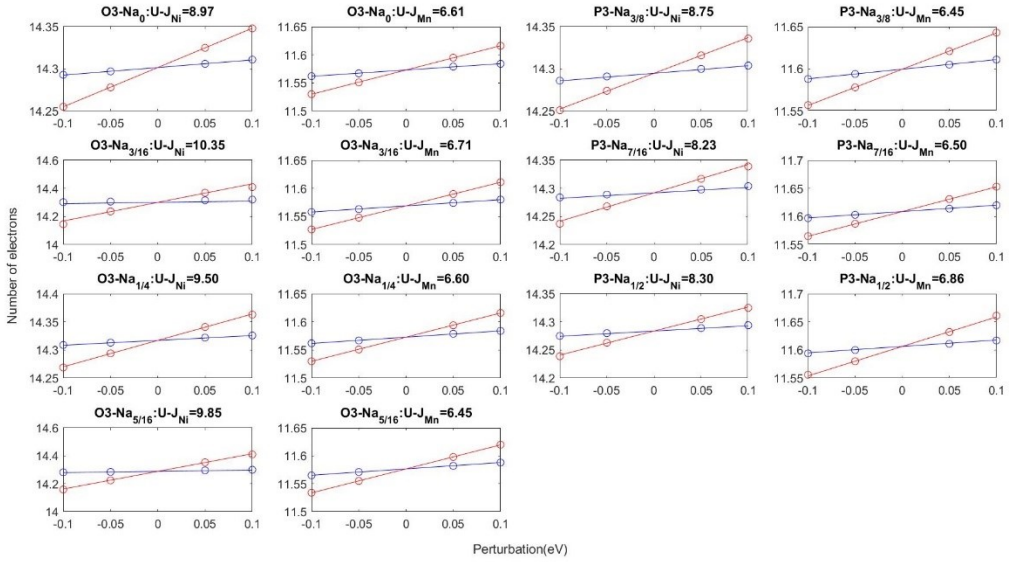

Figure S 14. Effective U-J values calculated for the P-O series using the linear response method[5]. Namely, a small perturbation (dv) is added on an arbitrary Ni/Mn atom for self-consistent (SF) and non-self-consistent (NSF) electron densities change (dn) on that atom to be calculated. The effective interaction parameter U-J values, or simply U values are estimated through:

$$U = \left({}^{dv}/_{dn}\right)_{NSF} - \left({}^{dv}/_{dn}\right)_{SF}$$

[5] Cococcioni, M., and De Gironcoli, S. (2005). Linear response approach to the calculation of the effective interaction parameters in the LDA+U method. Phys. Rev. B - Condens. Matter Mater. Phys. *71*, 1–16.

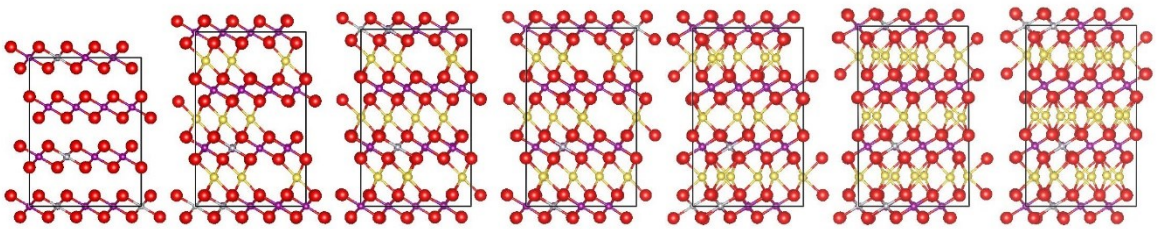

Figure S 15. Calculated structures viewed along *a* axis after ionic relaxation of the P-O series. See main text for an explanation of the notation. From left: O3Na0, O3Na3/16, O3Na1/4, O3Na5/16, P3Na3/8, P3Na7/16, P3Na1/2. Oxygen (red), transition metal (purple), sodium (yellow).

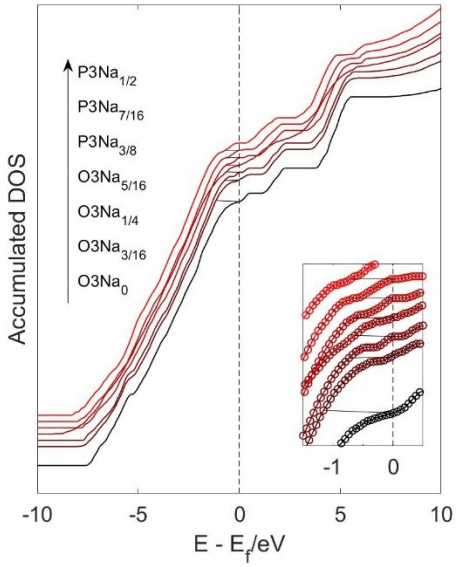

Figure S 16. Accumulated densities-of-states for the P-O series showing how the "band top" ranges of states were chosen.

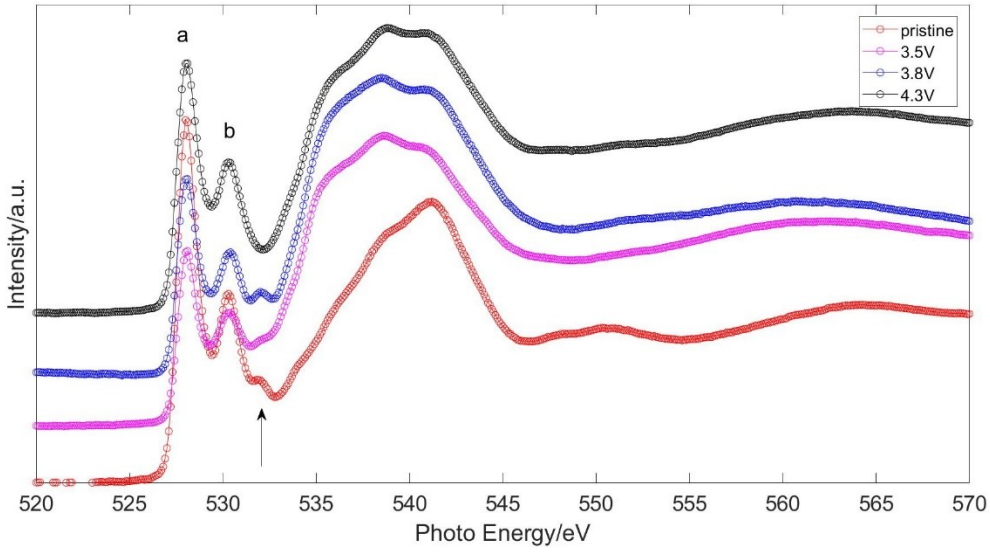

Figure S 17. O K-edge X-ray absorption spectra of pristine and charged samples. Linear backgrounds were subtracted according to the 510-520 eV signals and normalizations were done afterwards.

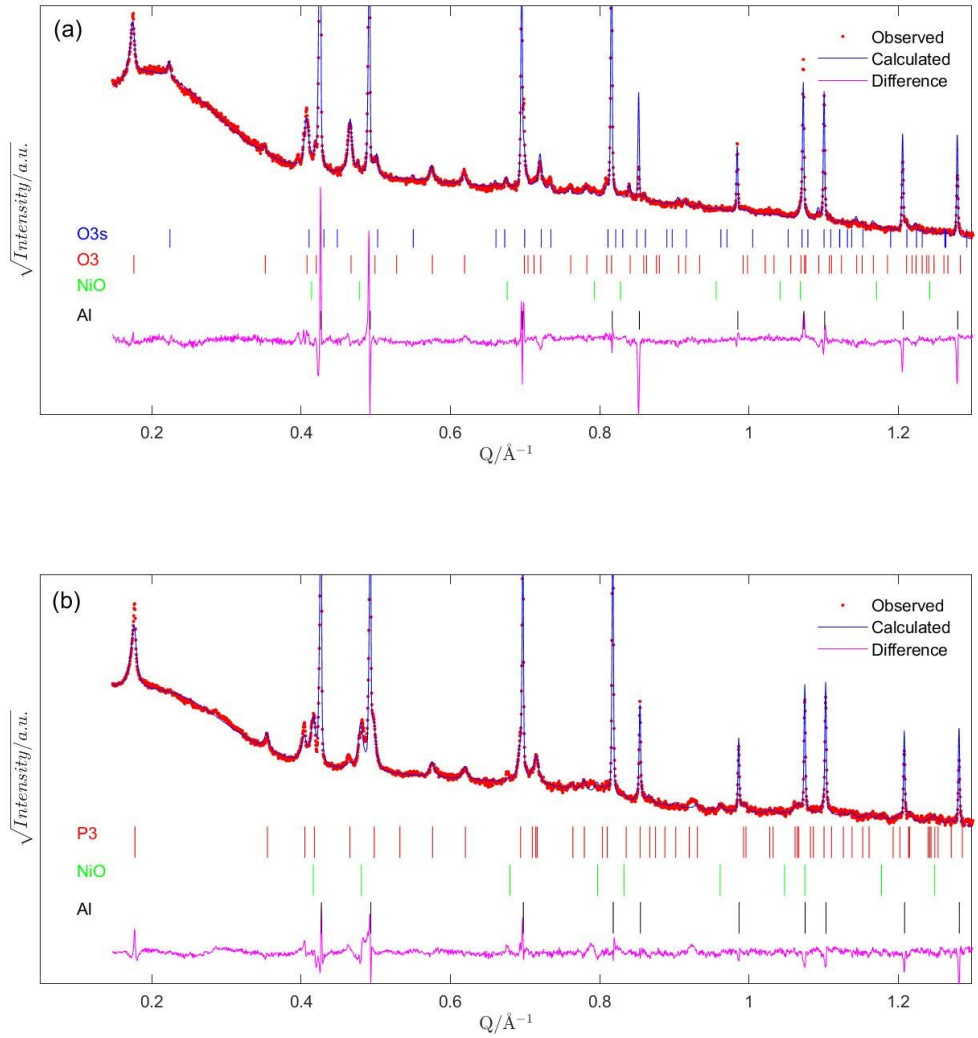

Figure S 18. Lab XRD data and Rietveld refinement of the *ex situ* samples of the P3-type $Na_{0.5}Ni_{0.25}Mn_{0.75}O_2$ material at state of charge 4.3 V (a) and 2.5 V (b) vs. Na^+/Na after 20 cycles at 10 mA/g, with the main relevant phase being O3 and P3 phase separately. A small amount of residue O3s phase is found at 4.3 V but not 2.5 V, even though the electrochemical reaction O3→O3s is thought to disappear as shown in the Figure 2(b) in the main article. This shows that O3→O3s reaction might still be achievable, but with growing polarization. All reflections show larger FWHM than those of the pristine samples, implying decrease in crystallinity or/and increase in strain.

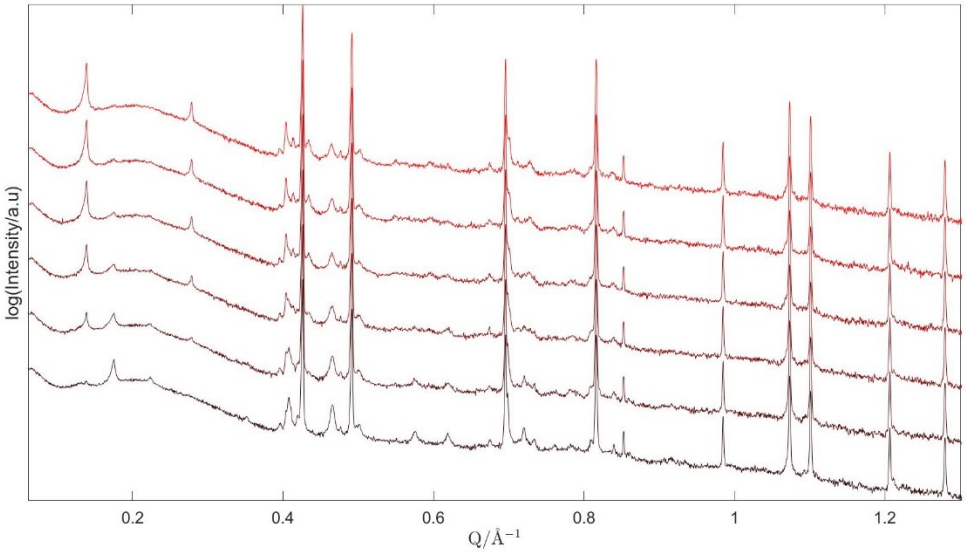

Figure S 19. Time evolution of lab XRD data of the *ex situ* samples of the P3-type $Na_{0.5}Ni_{0.25}Mn_{0.75}O_2$ material at state of charge 4.3 V vs. Na^+/Na after 20 cycles at 10 mA/g. All data were collected consecutively from bottom to top, with each data collected for an hour. Although the *ex situ* sample was sealed with Kapton tape and glue, the moisture somehow managed to infiltrate into the seal and transform the mixture of O3-O3s phases into a single phase of P3' phase with much greater interlayer spacing (*a*=2.86 Å, *c*= 21.46 Å as a preliminary refinement).

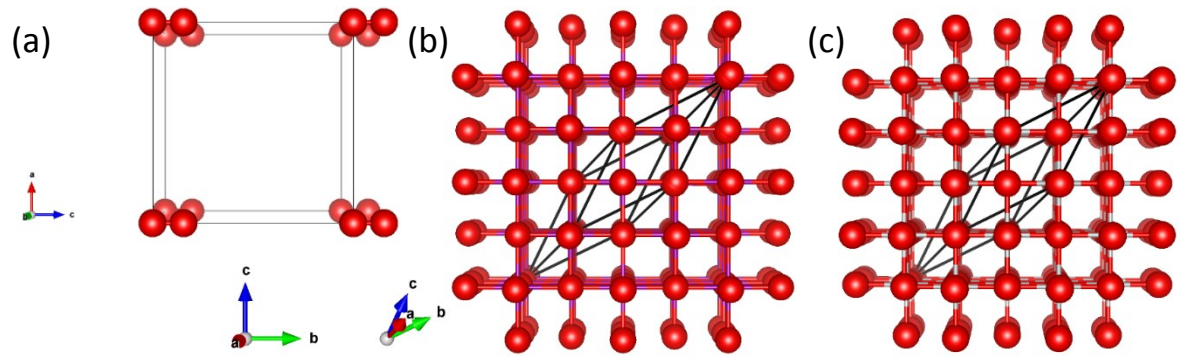

Figure S 20. Unit cells of relaxed structures of O2 dimer (a), MnO (b) and NiO (c) in antiferromagnetic configuration. The primitive cells containing 2 formula of MnO or NiO for calculation are also shown.

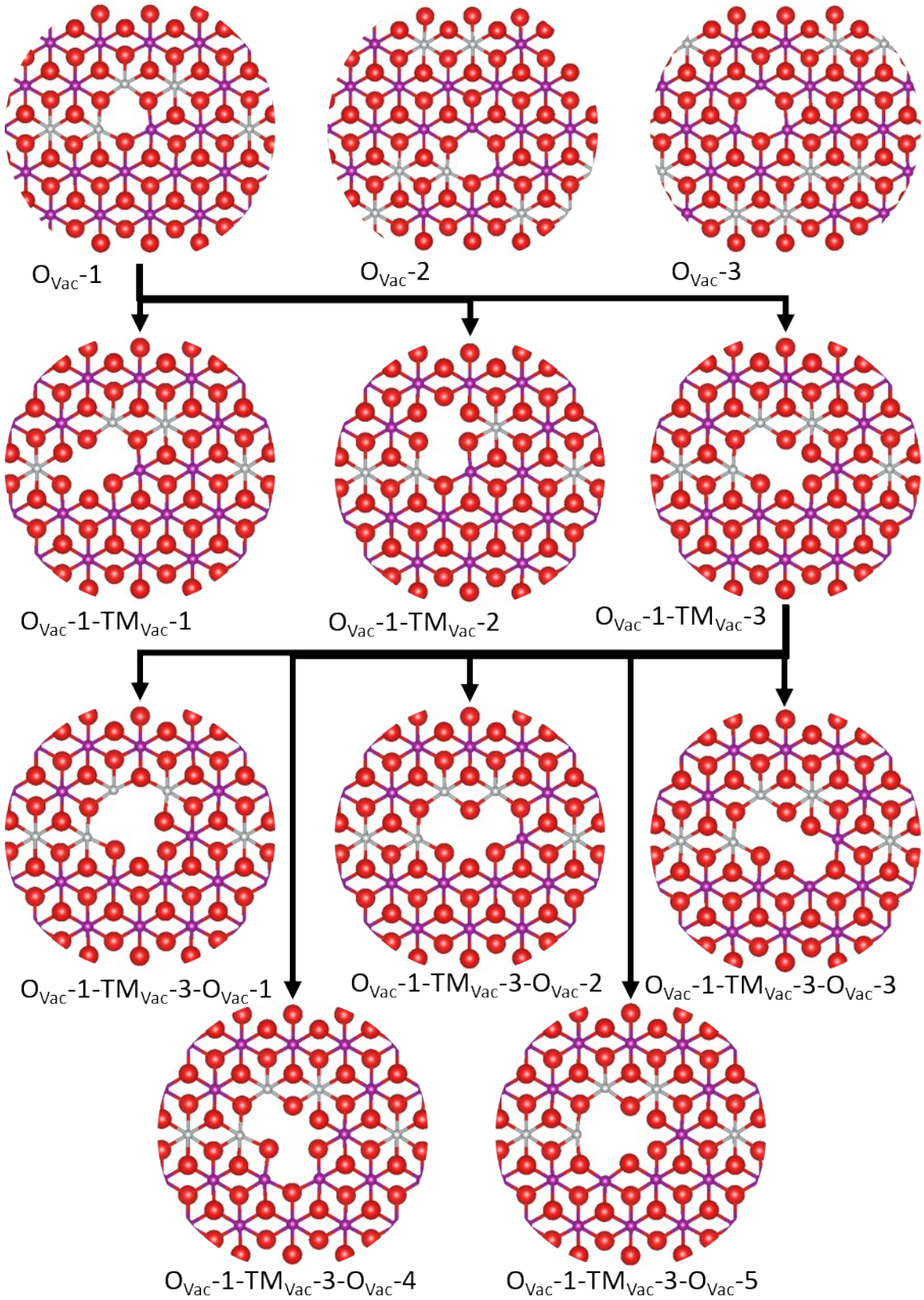

Figure S 21. Different types of one oxygen vacancy models (O_{Vac}-1, 2, 3), one oxygen vacancy one transition metal vacancy model derived from O_{Vac}-1 (O_{Vac}-1-TM_{Vac}-1, 2, 3), two oxygen vacancies one transition metal vacancy model derived from O_{Vac}-1-TM_{Vac}-3 (O_{Vac}-1-TM_{Vac}-3-O_{Vac}-1, 2, 3, 4, 5) are viewed along *c* axis with one layer of TMO_2 displayed (Red: O; purple: Mn; Grey: Ni).

Table S 10. Bond valence sum (BVS) maps for the P-O series structures. See main text for an explanation of the notation. Migration species are listed. Note that a calculated Na^+ BVS map for the O3Na0 structure containing no Na is meaningless; however, Ni^{2+} and Ni^{4+} BVS maps for O3Na0 and corresponding BVELs could be calculated. The isosurface value of each BVS map is the mobile ion's valence.

P3Na1/2 BVS Na^+	P3Na7/16 BVS Na^+	P3Na3/8 BVS Na^+	O3Na5/16 BVS Na^+
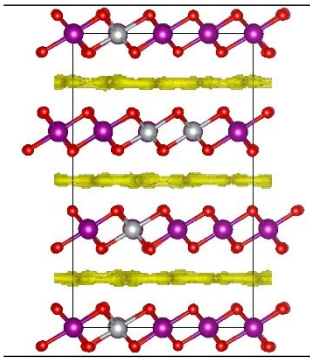	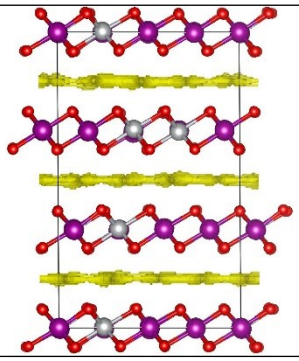	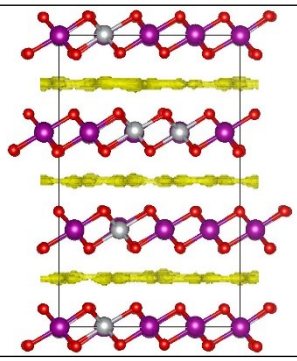	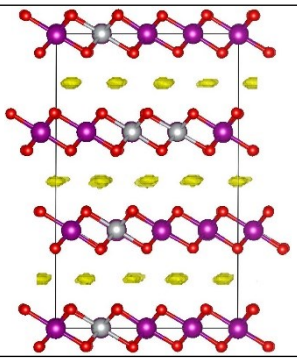
O3Na1/4 BVS Na^+	O3Na3/16 BVS Na^+	O3Na0 BVS Ni^{4+}	O3Na0 BVS Ni^{2+}
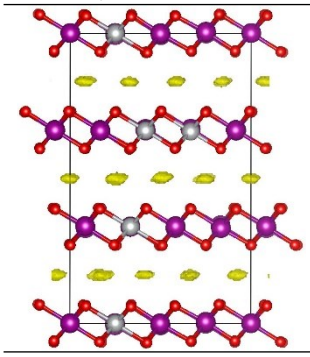	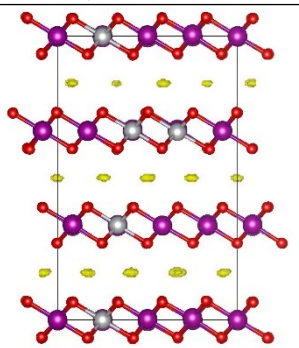	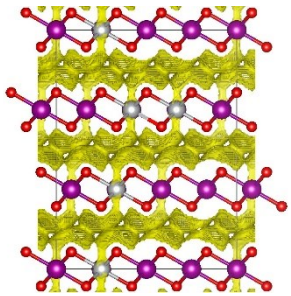	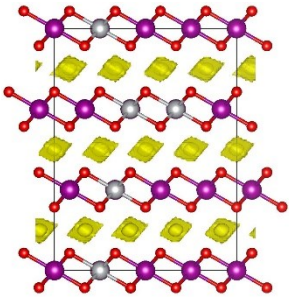

Table S 11. Bond valence energy landscapes for the P-O series structures. See main text for an explanation of the notation. Minimum energies E_{min} and minimum percolation energies E_{pcl} are listed. Note that a calculated Na^{+} BVELs for the O3Na0 structure containing no Na is meaningless; however, Ni^{2+} and Ni^{4+} BVELs for O3Na0 structure could be calculated. The isosurface value of each BVEL is E_{min} + E_{pcl} (eV).

P3Na1/2 BVEL E_{min}=-3.53; E_{pcl}=0.78	P3Na7/16 BVEL E_{min}=-3.52; E_{pcl}=0.81	P3Na3/8 BVEL E_{min}=-3.54; E_{pcl}=0.88	O3Na5/16 BVEL E_{min}=-3.46; E_{pcl}=2.62
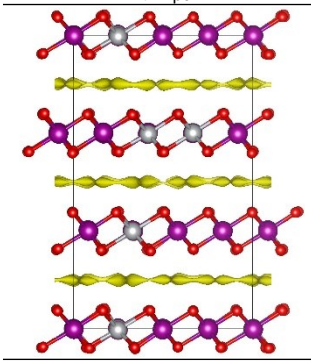	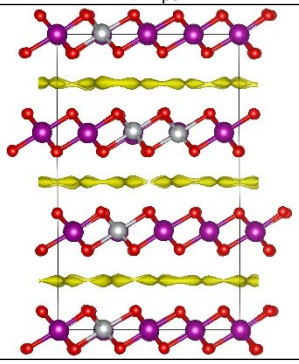	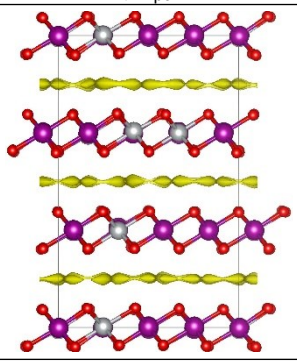	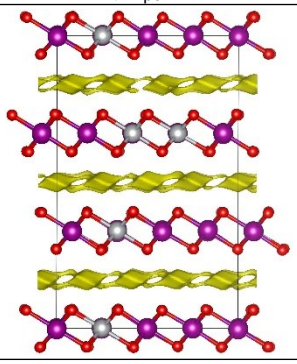
O3Na1/4 BVEL E_{min}=-3.45; E_{pcl}=2.62	O3Na3/16 BVEL E_{min}=-3.40; E_{pcl}=3.11	O3Na0 BVEL E_{min}=-5.72; E_{pcl}=1.61	O3Na0 BVEL E_{min}=-2.94; E_{pcl}=2.17
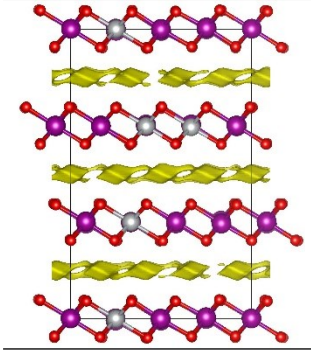	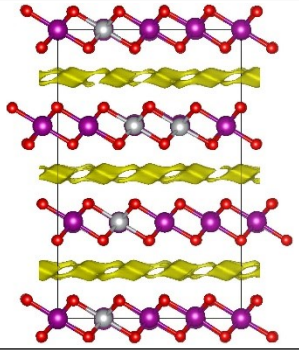	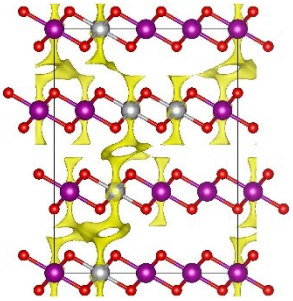	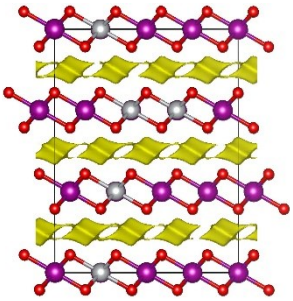

2, Mathematical proof of the effective equivalence and relationship between our simple linear model and the cluster expansion method

We start with the following mathematical description of the energy of a system based on the cluster expansion method taken from[6]:

$$E^{CE}(\sigma) = \bar{\Pi}(\sigma) \cdot J^{CE} = \sum_{\alpha} \bar{\Pi}_{\alpha}(\sigma) J_{\alpha}^{CE}$$

$$\sigma_i \in 1, -1$$

$$-1 \leq \bar{\Pi}_{\alpha}(\sigma) \leq 1$$

Where E^{CE} is the energy according to the cluster expansion method, σ is the ionic configuration, α is the type of cluster expansion configuration (referring to a specific type of cluster configuration), $\bar{\Pi}_{\alpha}(\sigma)$ refers to the so-called correlation matrix elements which accounts for the multiplicity of different types of configurations and J_{α} refers to the 'effective interaction strength' of each different type of cluster. The individual components of the occupancy vector σ_i have values of 1 and -1 representing occupancy and non-occupancy or two different types of occupancy respectively.

This equation is very similar to the simple linear model described in the main paper for calculating the energy as shown below. If we start from the linear regression equation, substitute in the new variable names from above and then neglect errors, we can write:

$$E^{LM}(\mu) = X(\mu) \cdot \beta + \varepsilon(\mu) \cong N X(\mu) \cdot J^{LM} = N \sum_{\alpha} X_{\alpha}(\mu) J_{\alpha}^{LM}$$

$$\beta = N J^{LM}$$

$$\mu_i \in 0,1$$

Where E^{LM} refers to the energy predicted by the linear model, $X_{\alpha}(\mu)$ refers to the count of the number of interactions of cluster type α divided by N in the given configuration μ and J_{α}^{LM} refers to the 'effective interaction strength' of each different type of cluster as above. N is a scaling factor which represents **the total number of partially occupant sites** in the system and is defined in the same way as for the cluster expansion method. This scaling factor is introduced to further improve the similarity between these two methods. $N J_{\alpha}^{LM}$ is equivalent to β from the main text. In this case, a different notation is used for the occupancy vector μ in that the values of 1 and 0 are used to represent occupancy and vacancy respectively, or in the case of Ni/Mn sites, occupancy of the site by a nickel or manganese atom respectively.

Both $X_{\alpha}(\mu)$ and $\bar{\Pi}_{\alpha}(\sigma)$ are sums over different types of cluster configurations but are defined slightly differently as described below. In our model, we only considered a linear model which includes diatomic interactions between neighbours as well as the total energy of the structure. We can write the equation for $X_{\alpha}(\mu)$, the total number of interactions divided by N, as follows:

$$X_{\alpha}(\mu) = \frac{1}{N} \sum_{\alpha \equiv \gamma} \prod_{i \in \gamma} \mu_i$$

$$\mu_i \in 0,1$$

$$\alpha \supset \gamma$$

[6] https://th.fhi-berlin.mpg.de/sitesub/meetings/dft-workshop-2016/uploads/Meeting/Tutorial_7_2016.pdf

In this notation, γ is an individual cluster of type α consisting of a group of specific atoms. In this notation, the inner multiplication runs over the positions in an individual cluster γ of type α and the outer summation performs addition of all clusters of type α over the whole crystal structure. In this case, only fully occupied clusters of type γ actually contribute to the total summation as they have no zeros. These formulas for the contents of the linear model equations include the N scaling factor which compensates for the total number of particles in a unit cell or chemical formula and also improves mathematical agreement between the cluster expansion and linear model methods.

The cluster expansion correlation matrix is defined in a slightly different way which is more salient for use in further studies of statistical mechanics as follows:

$$\bar{\Pi}_{\alpha}(\sigma) = \frac{1}{N}\sum_{\alpha \equiv \gamma}\prod_{i \in \gamma}\sigma_i$$

$$\sigma_i \in 1, -1$$

$$\alpha \supset \gamma$$

In this case, σ is a vector representing the state of the system. When a site is not occupied or if the cluster expansion method is modelling two different types of atoms, the possible value of σ_i of -1 means that these terms do not disappear in the summation and product expansions. We expect that this derivation can be expanded to the n[th] order and write out the expansion of these equations up to the second order as follows:

$$0^{th}\ order\text{:}\ \bar{\Pi}_{\alpha_0}(\sigma) = \frac{1}{N}\sum_{\alpha_0 \equiv \gamma_0} 1 = 1$$

$$1^{st}\ order\text{:}N\bar{\Pi}_{\alpha_1}(\sigma) = \sum_{\alpha_1 \equiv \gamma_1} \sigma_{\gamma 1}$$

$$2^{nd}\ order\text{:}N\bar{\Pi}_{\alpha_2}(\sigma) = \sum_{\alpha_2 \equiv \gamma_2} \sigma_{\gamma 2,1}\sigma_{\gamma 2,2}$$

In this notation, α_n represents a type of cluster of order n and γ_n represents a specific cluster atom. The σ_i and μ_i terms are directly related by the following equations:

$$\sigma_i = 2\mu_i - 1$$

$$\mu_i = \frac{1}{2}(\sigma_i + 1)$$

In the case of the linear model up to a di-atomic cluster, we can expand the expression for the site multiplicity up to the second order and re-express these equations as a function of σ then as a function of $\bar{\Pi}_{\alpha}(\sigma)$ using the above definitions as follows:

$$X_{\alpha}(\mu) = \frac{1}{N}\sum_{\alpha \equiv \gamma}\prod_{i \in \gamma}\mu_i$$

$$0^{th}\ order\text{:}X_{\alpha_0}(\mu(\sigma)) = \frac{1}{N}\sum_{\alpha_0 \equiv \gamma_0} 1 = 1 = \bar{\Pi}_{\alpha_0}(\sigma)$$

$$1^{st}\ order\text{:}2X_{\alpha_1}(\mu(\sigma)) = \frac{2}{N}\sum_{\alpha_1 \equiv \gamma_1} \mu_{\gamma} = \frac{1}{N}\sum_{\alpha_1 \equiv \gamma_1}\left(\sigma_{\gamma_1} + 1\right) = \frac{1}{N}\sum_{\alpha_1 \equiv \gamma_1}\sigma_{\gamma_1} + 1 = \bar{\Pi}_{\alpha_1}(\sigma) + 1$$

$2^{nd}\ order$: $4X_{\alpha_2}(\mu(\sigma))$

$$= \frac{4}{N}\sum_{\alpha_2 \equiv \gamma_2} \mu_{\gamma_{2,1}}\mu_{\gamma_{2,2}} = \frac{1}{N}\sum_{\alpha_2 \equiv \gamma_2}\left(\sigma_{\gamma_{2,1}}\sigma_{\gamma_{2,2}} + \sigma_{\gamma_{2,1}} + \sigma_{\gamma_{2,2}} + 1\right) = \frac{1}{N}\sum_{\alpha_2 \equiv \gamma_2}\sigma_{\gamma_{2,1}}\sigma_{\gamma_{2,2}} + \frac{1}{N}$$
$$\sum_{\alpha_2 \equiv \gamma_2}\left(\sigma_{\gamma_{2,1}} + \sigma_{\gamma_{2,2}}\right) + \frac{1}{N}\sum_{\alpha_2 \equiv \gamma_2} 1$$

$$= \bar{\Pi}_{\alpha_2}(\sigma) + \frac{n_{\alpha_2}}{N} m_{\alpha_2}\bar{\Pi}_{\alpha_1}(\sigma) + \frac{n_{\alpha_2}}{N} m_{\alpha_2}/2$$

m_{α_2} counts the multiplicity with respect to the specific cluster according to symmetry. n_{α_2} is the number of sites associated with the particular interaction. To understand the meaning of m_{α_2}, take the following four types of second order cluster for example. They are Na-Na first nearest interaction, Na-Na second nearest interaction, Na-TM first nearest interaction and TM-TM first nearest interaction. The solid balls represent sites which could be vacant or occupied, or species A or B in the case of ion mixing sites. For α_{Na-Na1}, $m_{\alpha_2} = 3$ and n_{α_2} is the number of Na sites. As second order interaction involves two atoms, the summation must be divided by 2. For α_{Na-Na2}, $m_{\alpha_2} = 6$ and n_{α_2} is also the number of Na ions. For α_{Na-Ni1}, $m_{\alpha_2} = 4$ and n_{α_2} is the number of Na sites and 2 fold of TM sites. For α_{TM-TM1}, $m_{\alpha_2} = 6$ and n_{α_2} is the number of TM sites.

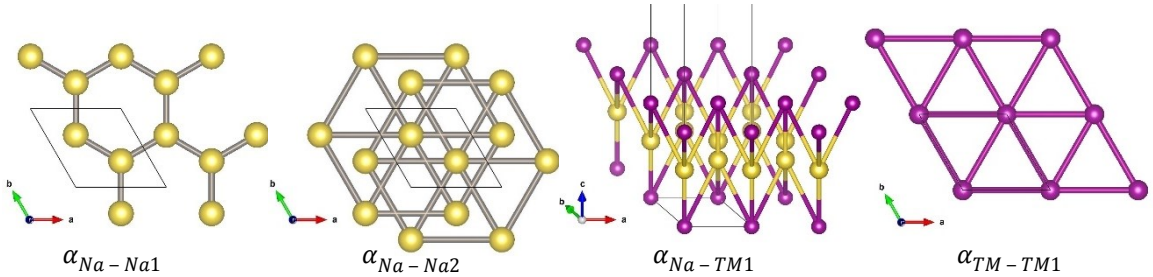

α_{Na-Na1} α_{Na-Na2} α_{Na-TM1} α_{TM-TM1}

We can re-write these equations as the following matrix equation:

$$\begin{bmatrix} X_{\alpha_0} \\ 2X_{\alpha_1} \\ 4X_{\alpha_2} \end{bmatrix} = \begin{bmatrix} 1 & 0 & 0 \\ 1 & 1 & 0 \\ \frac{m_{\alpha_2} n_{\alpha_2}}{2N} & \frac{m_{\alpha_2} n_{\alpha_2}}{N} & I \end{bmatrix} \begin{bmatrix} \bar{\Pi}_{\alpha_0} \\ \bar{\Pi}_{\alpha_1} \\ \bar{\Pi}_{\alpha_2} \end{bmatrix}$$

I is the identity matrix, whose dimension is decided by the number of the type of α_2 used. In more compact form:

$$X^T = P\Pi^T \text{ or } X = \bar{\Pi}P^T$$

$$P = \begin{bmatrix} 1 & 0 & 0 \\ 1/2 & 1/2 & 0 \\ m_{\alpha_2}/8 & m_{\alpha_2}/4 & I/4 \end{bmatrix}$$

From which we can see that $\bar{\Pi}_\alpha(\sigma)$ and $X_\alpha(\mu)$ are inter-transferrable via a linear relationship. By ignoring error term, we can obtain the relationship between J^{CE} and J^{LM} accordingly:

$E^{LM} = E^{CE}$

$X \cdot NJ^{LM} = \bar{\Pi} \cdot J^{CE}$

$\bar{\Pi} P^T \cdot NJ^{LM} = \bar{\Pi} \cdot J^{CE}$

$$P^T \cdot NJ^{LM} = J^{CE} \text{ or } NJ^{LM} = \left(P^T\right)^{-1} J^{CE}$$

$$E^{CE}(\sigma) = \sum_{\alpha} \bar{\Pi}_{\alpha}(\sigma) J_{\alpha}^{CE}$$

By solving the least square fit problem of either , the cluster expansion model or $E^{LM}(\mu) = \sum_{\alpha} X_{\alpha}(\mu)\beta_{\alpha}$, the simple linear model, we can obtain the coefficients of β_{α} and J_{α}^{CE} simultaneously.

(end of proof)